The Plenoptic Camera as a wavefront sensor for the European Solar Telescope (EST)

Luis F. Rodríguez-Ramos*[a], Yolanda Martín[a], José J. Díaz[a], J. Piqueras[a], J. M. Rodríguez-Ramos [b]

[a]Institute of Astrophysics of the Canary Islands, Tenerife, SPAIN
[b]University of La Laguna, Tenerife, SPAIN

ABSTRACT

The plenoptic wavefront sensor combines measurements at pupil and image planes in order to obtain wavefront information from different points of view simultaneously, being capable to sample the volume above the telescope to extract the tomographic information of the atmospheric turbulence. After describing the working principle, a laboratory setup has been used for the verification of the capability of measuring the pupil plane wavefront. A comparative discussion with respect to other wavefront sensors is also included.

Keywords: adaptive optics, atmospheric turbulence tomography, solar adaptive optics, plenoptic camera

1. INTRODUCTION

The plenoptic wavefront sensor, also known as the plenoptic camera or the CAFADIS camera, was originally created to allow the capture of the "Light Field" (LF) [1], a concept extremely useful in computer graphics where most of the optics are treated using exclusively the geometric paradigm. Basically the Light Field is a four-variable volume representation of all rays and their directions, and thus allows the creation by synthesis of the image as seen from virtually any point of view.

The history of the search for this description is really old, and references can be found in the very early beginning of the twentieth century, where F. Ives (1903) described a system with an array of pinholes at the focal plane or Lippmann (1908) Nobel prize laureate who described the first Light Field capturing device [2][3]. Modern light field description was stated by Adelson and Wang (1992)[4], and a significant step forward was done by Ren Ng (2005) [5] who built a working system and established a four-dimensional Fourier view of the imaging process. Recently, Georgiev (2009)[6] has introduced a number of diffraction considerations and defined the plenoptic camera 2.0.

The use of the plenoptic (CAFADIS) camera for real-time 3D cameras has been patented at the University of La Laguna (Spain) by one of the authors [7], exploiting the capability of refocusing at several distances and selecting the best focus as the distance to the object.

The use of plenoptic optics for wavefront measurement was described by Clare and Lane (2005) [8], for the case of point sources. We describe in this paper the use of the plenoptic camera as a wavefront sensor, especially adequate for computing the tomography of the atmospheric turbulence for adaptive optics in solar telescopes. After a description of the sensor and the required processing, the results of laboratory tests are presented, which clearly show the viability of the system for pupil plane wavefront measurement.

2. DESCRIPTION OF THE PLENOPTIC WAVEFRONT SENSOR

A microlens array with the same f-number than the telescope is placed at its focus (fig 1), in such a way that many pupil images are obtained at the detector, each of them representing a slightly different point of view. The use of the same f-number guarantees that the size of the image of the pupil is as big as possible, without overlapping with its neighbor, providing thus optimum use of the detector surface. An example of a plenoptic image obtained at the Vacuum Tube Telescope (VTT, Canary Islands, Spain) is shown in fig. 2, depicting an array of 15x19 microlenses imaged on a 1024x1280 uEye CMOS Camera. The spider support for the secondary mirror can be easily identified, together with some vignetting at the lower left side, created by the telescope configuration at the moment of the data acquisition.

*lrr@iac.es; phone +34 922 605 200; fax +34 922 605 200; www.iac.es

In order to understand the behavior of the plenoptic wavefront sensor, it is important to identify the direct relationship existing between every pupil point and its corresponding image for each microlens. As shown in fig 3, every pupil coordinate is imaged through each microlens in a way that all rays passing through the indicated square will arrive to one of the pupil images, depending only on the angle of arrival. This fact clearly indicates that the image that would be obtained if the pupil were restricted to this small square can be reconstructed by post-processing the plenoptic image, selecting the value of the corresponding coordinate at every microlens and building an image with all of them.

If diffraction considerations are introduced in addition to geometric optics, as stated by Clare and Lane [8], the image obtained using this post-processing is really the result of the convolution of the geometric image with the transfer function of the microlens, which basically implies a low pass blurring equivalent to the well known diffraction limiting effects found when imaging through a finite aperture. These effects however will be neglected along this article except when evaluating the maximum resolution attainable in the pupil plane wavefront measurement.
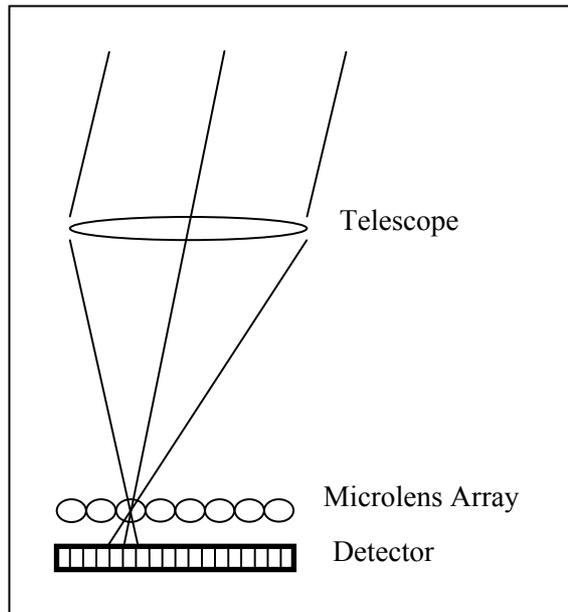

Fig. 1. Outline of the plenoptic camera used as wavefront sensor. A microlens array is located at the telescope focus, instead of in some pupil plane as required for the Shack-Hartmann (SH) sensor. If the f-numbers of both telescope and microlens are the same, the detector will be filled up with images of the pupil of maximum size without overlapping.

With this scheme, both pupil and image planes are sampled simultaneously, and later processing may extract relevant information coming from the volume above the telescope. The simplest case is the wavefront at the pupil, which can be extracted from the relative displacement of the recomposed images from every pupil coordinate, specifically for solar adaptive optics, in the following way:

a) To compensate the plenoptic image from zero-level and differential pixel response (bias and flat), using calibration information regarding the optical and electronics system.

b) To generate the images corresponding to every pupil coordinate, using the resolution and/or filtering adequate to the desired sampling scheme.

c) To compute the cross-correlation of every image with respect to one of them, in order to evaluate the relative average tilt of the pupil plane wavefront. The position of the peak of the correlation is computed with sub-pixel resolution using quadratic interpolation between the maximum correlation value and its neighbors.

d) To estimate the phase surface from the local derivatives using a suitable algorithm, like the Hudgin iterative reconstructor. [See J. Díaz et al, this conference].

This arrangement will be especially useful when extended objects are imaged, and the case of solar granulation will be specifically addressed.
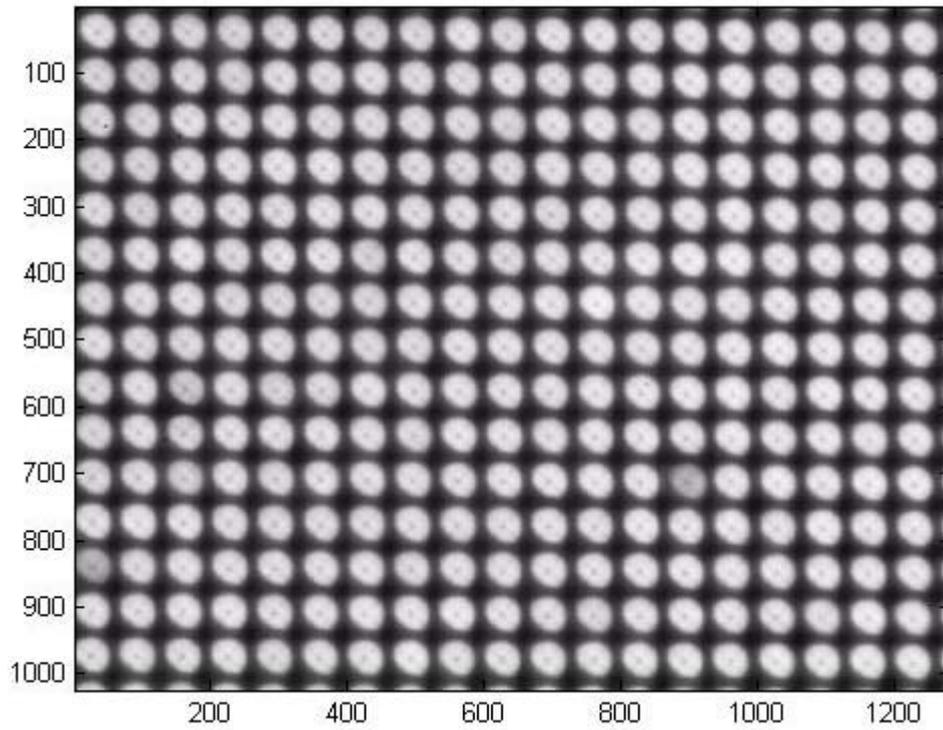

Fig. 2. Example of plenoptic image of the Sun on a plenoptic camera of 19 x 15 microlenses, using a detector of 1280 x 1024 pixels at the VTT telescope (Observatorio del Teide, Canary Islands, Spain)
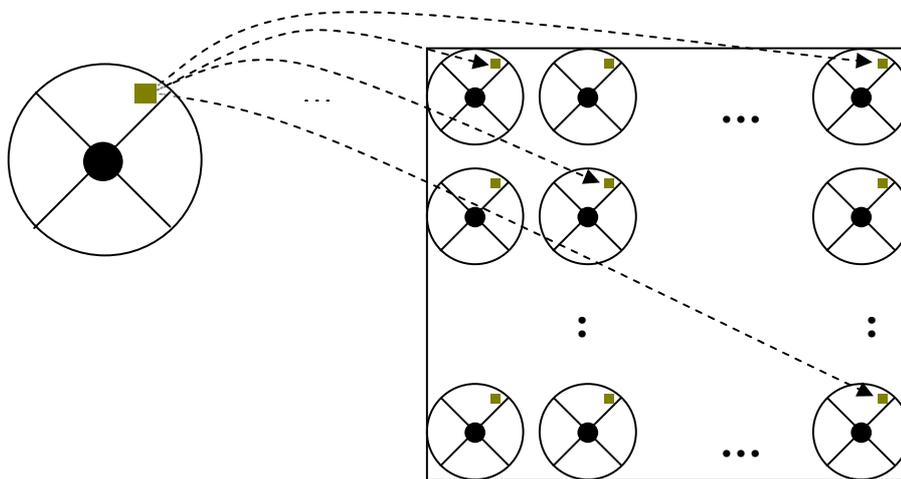

Fig. 3. Correspondence between pupil and pupil images. Every pupil coordinate is re-imaged on the corresponding position of each pupil image, depending on the arriving angle of the incoming ray.

3. PUPIL PLANE RESOLUTION LIMIT

It is well known that at least an aperture in the range of 70-100 milimeters is needed to obtain a reasonably good image of the solar granulation, which will be used as a correlation guide for estimating image displacements and then converted to wavefront tilts. When a Shack-Hartmann (SH) wavefront sensor is used, this limit will directly impose a maximum resolution level in the pupil wavefront measurement, due to the fact that no more than

$$N_D = \frac{D}{D_{SH}}$$

(1)

subpupils can be allocated at the system entrance diameter, if solar granulation is expected to be present at the resulting subpupil image. (Let D be the telescope diameter and D_{SH} the minimum aperture acceptable to have solar granulation in the image).

This number could become a serious limit when the adaptive optics tries to reach superb working figures, because it will affect directly at the quality of the reconstruction (or the AO overall figures) governing the fitting error of the measured wavefront. This limit will turn on a maximum of ≈7 wavefront pupil samples (in diameter) in a telescope like VTT (Teide Observatory), or 40 in a 4-m telescope (EST). In order to check if the plenoptic wavefront sensor could be used to overcome this limitation, the maximum resolution achievable will be analysed in this section.

Solar granulation information is located at high spatial frequencies, with very low contrast unfortunately. An optical imaging system with a minimum bandwidth is needed to provide sufficient throughput at those spatial frequencies, being this bandwidth represented by the cut-off frequency of the optical transfer function of the circular aperture. This cut-off spatial frequency is [9]:

$$\rho_c = \frac{D}{\lambda f}$$

(2)

Being D the aperture, λ the wavelength of the light and f the focal length of the imaging system. In our case, the value of the cut-off frequency adequate for the solar granulation will be given by the specific values of D_{SH} (maximum SH aperture) and f_T (Telescope focal length):

$$\rho_c = \frac{D_{SH}}{\lambda f_T}$$

(3)

As described previously, the virtual image corresponding to any aperture can be synthesized from the plenoptic image by selecting one pixel from each microlens. In order to have some level of solar granulation to correlate with, these spatial frequencies shall be present and adequately sampled, in a similar way that would happen to a SH sensor. Using the Shannon theorem, correct representation of the solar granulation spatial frequencies will require a sampling of twice these frequencies ($2\rho_c$) and thus will impose a limit on the separation of the microlenses: The microlenses should not be separated at the focal plane by more than $1/2\rho_c$ meters (or microns) and thus they can not be bigger than this size.
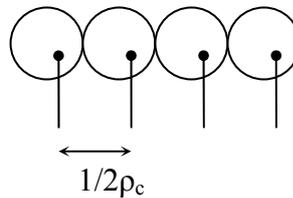

Fig. 4. The synthesized image is built after selecting one pixel from every microlens. High spatial frequencies containing granulation information will only be present at the reconstructed image if the separation between microlenses is less than $1/2\rho_c$, being ρ_c the spatial frequency of the solar granulation.

Using this scheme, it can be easily shown that the maximum microlens size is related to the minimum SH subpupil by:

$$D_{\mu L} = \frac{1}{2\rho_c} = \frac{\lambda f_T}{2D_{SH}} \tag{4}$$

Looking at the expression giving the maximum $D_{\mu L}$ (4), it should be concluded that a bigger focal length will allow for bigger microlenses and thus better pupil imaging, because the image of the pupil will also be affected by the resolution limit blurring, as shown next.

Considering now the propagation through the microlenses, using again the system transmission of a circular aperture, the maximum available spatial frequency at the pupil plane will be

$$F_c = \frac{D_{\mu L}}{\lambda f_{\mu L}} \tag{5}$$

And thus the sampling pitch at the pupil plane needed for grasping all the information available will be (double):

$$\delta_{pupil} = \frac{\lambda f_{\mu L}}{2D_{\mu L}} \tag{6}$$

Being this time the microlens focal length and its diameter the parameters of the equation. Substituting the microlens diameter previously calculated, the maximum pupil sampling can be obtained, i.e, the minimum separation of pupil samples where the wavefront information can be measured independently.

$$\delta_{pupil} = \frac{\lambda f_{\mu L}}{2D_{\mu L}} = \frac{\lambda f_{\mu L}}{2\frac{\lambda f_T}{2D_{SH}}} = D_{SH}\frac{f_{\mu L}}{f_T} \tag{7}$$

Which shows that the minimum distance between pupil measurements is the one of the SH sensor times the ratio of the focals (microlens/telescope). Finally, if the condition of the plenoptic camera for best use of the detector is used [5] (Basically means that pupil images equal the microlens pitch)

$$\frac{f_T}{D_T} = \frac{f_{\mu L}}{D_{\mu L}} \tag{8}$$

…it can be directly deduced that the separation between pupil measurements is:

$$\delta_{pupil} = D_{\mu L}\frac{D_{SH}}{D_T} \tag{9}$$

…which is exactly the same amount provided by the SH wavefront sensor, because the ratio D_{SH}/D_T is the inverse of the number of SH subpupils in a telescope diameter, and is multiplying the microlens diameter, which represents the size of the pupil image.

4. LABORATORY PUPIL WAVEFRONT RECOVERY

In order to verify experimentally the capability of the plenoptic camera for acting as a wavefront sensor, the optical setup described in fig 5 was built. The underlying idea was to have a method for varying the pupil wavefront under user control, and then verify up to what point the plenoptic sensor was capable of extract the generated wavefront. A deformable mirror re-imaged on the aperture was used for that purpose.
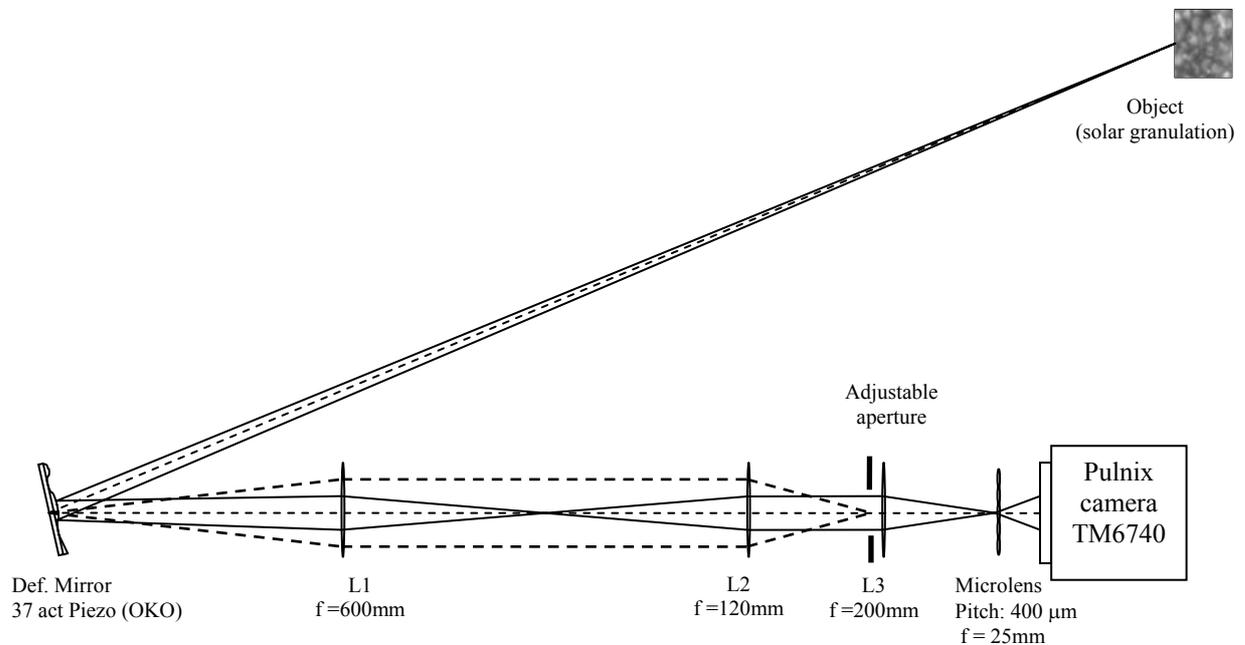

Fig. 5. Optical setup used for verifying the pupil plane wavefront recovery by the plenoptic wavefront sensor. Plenoptic camera is built using a 200 mm focal length doublet (L3) plus the microlens array. An extended object simulating solar granulation (or any other with high spatial frequency content) is collimated by L1 and L2 to be imaged by the plenoptic camera. At the same time the pair L1+L2 reimages the deformable mirror surface at the entrance pupil, allowing for direct control of the phase at this point.

The plenoptic camera was built by combining a 200 mm focal length acromatic doublet (L3) with a microlens array from Adaptive Optics Associated, with 400 micron pitch and 25 mm focal length. An adjustable aperture was used to reduce the aperture to the required value in order to have reasonable matched f-numbers (3 mm aprox). The iris was located very close to the lens surface, practically glued to it. The plenoptic image was captured by a fast CCD gig-E camera (Pulnix TM6740), having 640x480 squared pixels of 7.4 microns. Plenoptic images captured with this optical setup contain 10x8 pupil images, as shown in fig. 6.

A number of objects were collimated to be imaged by the plenoptic camera, going from a very simple cross to a solar granulation photograph, and also a blank reference for flat fielding and microlens centres computation. Collimation is obtained using L1 (f = 600 mm) and L2 (f = 120mm) which also create a reduced image of the deformable mirror (25 mm, 37 piezo actuators from OKOTECH) on the aperture, which provides phase control at this point.
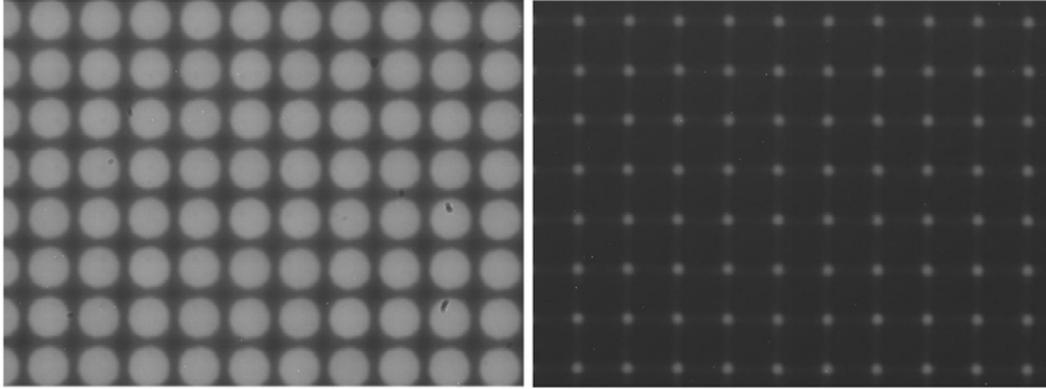
Fig. 6. Images showing the flat blank image of all pupils (left) and the result of reducing the aperture to its physical minimum to find the position of the centers of the microlenses, which will be the reference for all pupil coordinates.

Fig. 7 depicts plenoptic images of a very simple object, a cross, viewed through the optical setup with two different positions of the deformable mirror. All actuators were set at the intermediate value, and actuator #14 was changed from minimum actuation to maximum stroke. It should be noted that the intermediate value in all actuators does not mean a flat mirror shape, due to residual flatness error during mirror manufacturing.
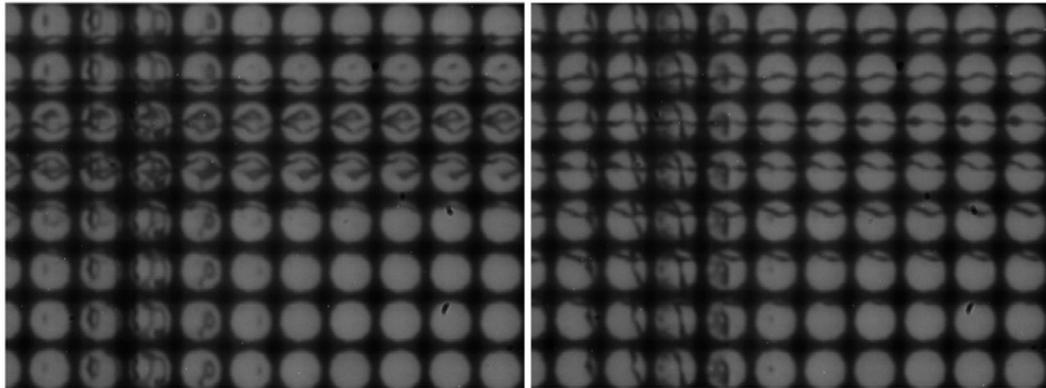

Fig. 7. Plenoptic images of a cross at two different positions of actuator #14. Note that pupil images are not uniformly illuminated due to the finite distance to the object.

The plenoptic images of fig 7 are recomposed in fig 8, following the proposed scheme. A circular pupil is found in both cases, and when both images are compared with some detail, it can be noticed that the movement of the cross depends on the pupil position sampled, with almost no change nearby the border and maximum towards the center of the pupil, where the actuator is located. This change is much more obvious when a movie of the movement of actuator #14 is recorded and played back. Correlation computation would follow, but it will not add any more insight to the visual procedure and will not be included in this article.
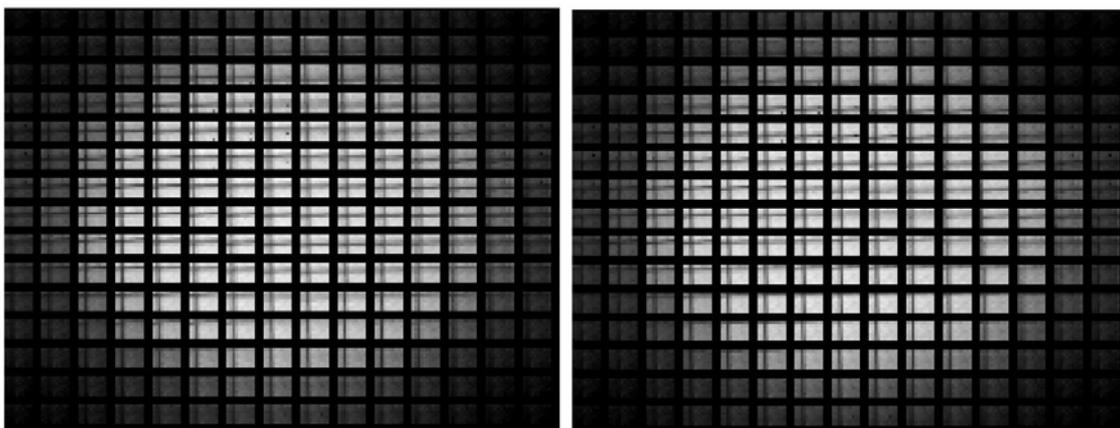
Fig. 8. Recomposed pupil images of a cross, grabbed at two different positions of actuator #14. Note that maximum object displacement is found at the center of the pupil, and its direction and magnitude vary according to the pupil coordinate being sampled.

5. COMPARISON WITH OTHER WAVEFRONT SENSORS

Plenoptic wavefront sensor could be considered as a generalization of the pyramid wavefront sensor, in the sense that images of the pupil are used for computing the wavefront, but without any moving part and to be used with extended or constellations of objects. The direct comparison should be with respect to the Wide Field Shack Hartmann wavefront sensor also used for solar adaptive optics, where tomography is computed after examining several zones of a wide field of view on each subpupil. The main advantage is the absence of field stop and pupil reimage, simplifying the optics needed. Also the capability of synthesizing virtually any aperture to work with allows adapting the adaptive optics system to different levels of turbulence, by changing –even in real time- the order of the system in accordance with those levels. The price to be paid is the extra blurring induced on the pupil plane wavefront estimation by the finite microlens diameter, and of course the extra processing needed.

However, a very interesting capability of the plenoptic camera comes from the possibility of obtaining images focused to any height (or distance) by properly selecting the adequate pixels from the microlenses images. This is a very powerful tool to be further investigated in relation with the atmospheric turbulence tomography computation.

6. CONCLUSIONS, ACKNOWLEDGEMENTS AND FUTURE WORK

The plenoptic wavefront sensor has been introduced and described, together with the analysis of its applicability to solar adaptive optics. Despite its simplicity, it can be used for pupil plane wavefront measurement to obtain the same resolution than the Shack-Harmann sensor, with the extra blurring caused by the finite (and normally small) size of the microlenses. Using a direct laboratory measurement, it has been shown that pupil plane wavefront can be measured by the plenoptic camera.

Future work includes the installation of a plenoptic camera at the VTT telescope, (Observatorio del Teide, Canary Islands, Spain) expected by summer 2009. A 2048 x 2048 pixel camera will be used for this purpose, with appropriate sampling of 10x10 pixels per pupil image. Real-time processing of the plenoptic sensor for solar images is also being developed, and a conceptual has already been presented at the AO4ELT Congress held in Paris last June.

REFERENCES

[1] Ng, R., "Fourier Slice Photography", Stanford University, (2005).

[2] Lippmann,M. G.,"Épreuves réversibles donnant la sensation du relief", J. de Phys. 4,VII,(1908).

[3] Lippmann, G., "La photographie intégrale". Comptes-Rendus, Académie des Sciences 146, 446-551 (1908).

[4] Adelson, T., and Wang, J. Y. A., "Single lens stereo with a plenoptic camera", IEEE Transactions on Pattern Analysis and Machine Intelligence 14, 2(Feb), 99-106, (1992).

[5] Ng, R. et al, "Light field photography with a hand-held plenoptic camera", Tech. Rep. CSTR 2005-02, Stanford Computer Science, (2005).

[6] Georgiev, T., Lumsdaine, A., "Superresolution with Plenoptic Camera 2.0", Adobe Tech Report, April (2009)

[7] Rodríguez-Ramos, J. M. International Patents ES200800126 ES200600210 (2006)

[8] Richard M. Clare and Richard G. Lane, "Wave-front sensing from subdivision of the focal plane with a lenslet array," J. Opt. Soc. Am. A 22, 117-125 (2005)

[9] Goodman, J.W., "Introduction to Fourier Optics", 2nd Edition, McGraw-Hill, (1996)